ELSEVIER

Fusion Engineering and Design 42 (1998) 555–561

Fusion Engineering and Design

Scaling criteria for IFE liquid wall protection scheme simulation

Alice Ying *, Mohamed Abdou

Mechanical and Aerospace Engineering Department, University of California, Los Angeles, CA 90095-1597, USA

Abstract

Applicability of experimental results to a full-size system depends on the scaling criteria on which the test article/fluid medium is used. This paper presents a careful review and assessment of a number of key parameters which influence fluid stability phenomena relevant to the IFE wall protection schemes, and provides guidance for future simulation experiments. The analysis shows that the non-dimensional jet surface ripple size can be reproduced by simultaneously preserving prototypical jet Reynolds and Weber numbers. The results show the difficulties of using water as a simulant for liquid protectants in experiments for evaluating IFE thin and thick liquid wall protection schemes. The analysis also shows that a modified HTS salt seems a good simulant for Flibe and that liquid sodium a good simulant for liquid lead. However, in the absence of information on liquids other than water, serious questions remain concerning the issue of scaling. Nevertheless, to best utilizing the available R&D resources, further experiments should be performed using fluids with significantly lower vapor pressures, such as liquid metals or low-melting temperature salts or eutectics. © 1998 Elsevier Science S.A. All rights reserved.

1. Introduction

Concerns about the feasibility of IFE liquid wall protection schemes have stimulated research in the thermal hydraulics of liquid protection systems (M.J. Longeot, P.F. Peterson, personnel communication, 1996.) and Cavanaugh and Peterson [1]. Uncertainties associated with liquid wall protection concepts are: the required jet configurations for meeting the needed chamber conditions, the hydrodynamic stability of high Reynolds number jets exposed to turbulent fluctuations, and of falling film stability for given flow geometries [2–4]. The applicability of the experimental results to a full-size system depends on the scaling criteria on which the test article/fluid medium is designed. This paper presents a careful review and assessment of a number of key parameters which influence fluid stability phenomena relevant to the IFE wall protection schemes, and provides guidance for future simulation experiments. The purpose is to ensure that the results of these experiments are meaningful in evaluating the performance and improving the protection scheme designs for the cavity chamber. The jet concepts under investigation include: thick falling film/plane sheet jets, thin film, and inverted falling film jets with the working fluids of Flibe(Li_2BeF_4), lithium and lead. Discussions in the next section relate issues concerning thin film concepts, while the third section is devoted to issues concerning the thick liquid flow protection scheme. Since the unstable phenomena are the consequences of the fluid properties combined

* Corresponding author.

0920-3796/98/$19.00 © 1998 Elsevier Science S.A. All rights reserved.
PII S0920-3796(98)00135-5

Table 1
Reactor and experimental liquid property data

Liquid (melting T)	Temp.°C	Density (kg m^{-3})	Viscosity (kg m^{-1} s^{-1})	Surface tension (N m^{-1})	N_σ [Eq. (6)]
Reactor fluids					
Lithium (179°C)	500	482	0.34×10^{-3}	0.349	67 940
Flibe (460°C)	600	1963	6.78×10^{-3}	0.193	1106.88
Lead (327.4°C)	450	10 450	2.087×10^{-3}	0.438	21 235
Fluids used in experiments					
Sodium (97.8°C)	103.7	928	6.86×10^{-4}	0.2062	19 576.5
Potassium (63.7°C)	85	822.6	4.86×10^{-4}	0.086	12 387.6
Water	20	1000	1.06×10^{-3}	0.734	4280.0
Water	90	970	0.32×10^{-3}	0.617	16 400.0
KNO_3-$NaNO_3$(220°C)	220	1952	4.67×10^{-3}	0.122	1149

with operating flow regimes, the basic properties of the reactor liquids at relevant operating temperatures are summarized in Table 1 along with those of common liquids used in falling film and jet flow experiments at the relevant temperatures of the given experiment.

2. Thin film protection scheme

A thin film protection scheme refers to an IFE chamber design concept which utilizes a thin sacrificial layer of liquid supplied from a porous first wall structure to absorb the instantaneous X-ray and debris energy following a fusion pellet explosion. Different design studies have utilized this generic concept in different ways, the most recent being the Prometheus [2] and OSIRUS [3] conceptual designs.

2.1. Inverted falling film flow

One of the uncertainties associated with using thin films as a protection scheme in IFE relates to flows on inverted surfaces found within the reactor chamber. The stability of the film can be analyzed by looking at the wave activities on the film surface. For the thin laminar film flow such as found in the OSIRUS design, the most important parameter characterizing wave growth on film surface is the growth exponent (G). G can be written as [5]

$$G = \frac{u_0}{h}\gamma t \tag{1}$$

where

$$u_0 = \frac{gh^2}{2v}\sin\theta = \text{velocity at the free surface} \tag{2}$$

$$\gamma = \frac{2\alpha^2}{3\sin\theta}\left[\left(\frac{6}{5}\,\mathrm{Re}\sin\theta - \cos\theta\right) - \frac{\Gamma}{gh^2}\alpha^2\right] = \text{instability's growth rate} \tag{3}$$

and g and h are gravitational force and film thickness, respectively and t is the film traveling time (here, taken as 1/repetition rate = 0.2 s).

The parameters Γ end θ as in Eq. (3) are the kinematic surface tension and angle between the fluid surface and the horizontal plane. The wave frequency (α) and film Reynolds number (Re) are calculated as:

$$\alpha = 2\pi h/\lambda \tag{4}$$

and

$$\mathrm{Re} = \frac{\bar{u}}{v} = \frac{gh^3\sin\theta}{3v^2} \tag{5}$$

where λ is the wavelength and v is the kinematic viscosity.

The growth G is plotted versus wavelength (λ) for a film thickness of 300 μm at $\theta = 135°$ (corresponding to an inverted inclined surface of 45°) in Fig. 1 for Flibe, water, and KNO_3-$NaNO_3$ (50:50%) molten salt (modified HTS). The results show that for these cases the maximum growth

occurs at about the same wavelength. However, the growth of any disturbance for water film is at least one order of magnitude higher than that for Flibe film. Thus, a disturbance observed on water film surface is to be amplified much more quickly than that found on Flibe film surface. A more representative Flibe film wave growth can be produced by using modified HTS salt. The fluid has an advantage over Flibe because of its melting temperature of 220°C, instead of that more than 460°C for Flibe. The calculated limiting stable wavelength (any wavelength greater than the limiting wavelength grows with time) for different fluids at different film thickness are given in Fig. 2. For a thin film of 100 μm, water can handle a wave length disturbance of up to 3.4 cm while both Flibe and modified HTS of 1.5 cm. Furthermore, growth calculations show that a given disturbance of smaller than the limiting disturbance is much more strongly damped in water than in Flibe. As a result, it will be difficult to predict Flibe falling film behavior according to the experimental data for water. Another point to be noted as shown in Fig. 2 and from growth calculations (not shown) indicates that a small wave introduced on the lead film surface might violently disrupt the flow.

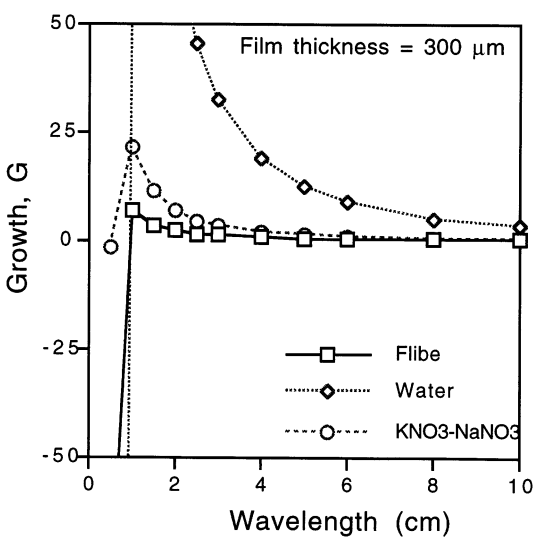

Fig. 1. Nondimensional growth versus wavelength for different working fluids.

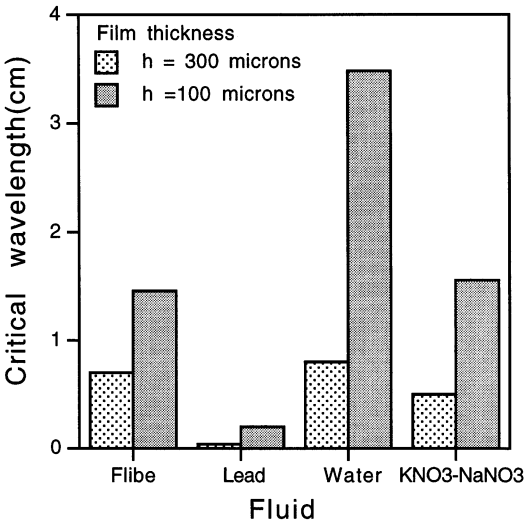

Fig. 2. Critical wavelength for different fluids in an inverted surface of 45°. (The surface is stable for wavelengths shorter than critical wavelength).

2.2. Wave characteristics of turbulent thin film and impact on film thickness

Modelling of turbulence in films is generally complicated by the wave activity at the film interface which results in severe variations of local film thickness and continuous longitudinal changes in the hydrodynamic structure of the falling film. (Note: uniformity of film thickness is viewed as one of the feasibility issues in the Prometheus design). The large waves continue to change shape as the liquid flows down the plate and some coalesce so that the frequency of the waves becomes irregular. In the course of discussion, the asymptotic solution to the falling film stability problem is used for experimental planning guidance.

One of the key nondimensional parameters impacting the characteristics of the waves that form on isothermal vertical falling films is the surface tension number (N_σ) defined as[6]

$$N_\sigma = \frac{\sigma}{\rho}\left[\frac{2}{\nu^4 g}\right]^{1/3} \tag{6}$$

where σ is the surface tension coefficient and ρ is the liquid density. For the liquid metals, the values of the surface tension number are appreciably

Table 2
Characteristics of expected jet surface protuberance curvature under reactor and simulant operating conditions

Operating parameter	HYLIFE-II	Scaled (Pure water)	Scaled (Water, reduced surface tension)	Experiments (Water)
Jet Reynolds number	2.43×10^5	2.43×10^5	2.43×10^5	1.043×10^6
Jet Weber number	1.03×10^5	1.03×10^5	1.03×10^5	1.469×10^5
Jet thickness (cm)	7	1.9	3.7	10
Jet velocity (m s^{-1})	12.0	20.4	10.2	10.28
Jet turbulence (m s^{-1}) [Eq. (8)]	0.5093	0.8658	0.4329	0.3636
Jet surface protuberance curvature (mm) [Eq. (10)] non-dimensional Jet	0.0643	0.017	0.0344	0.0782
Surface protuberance curvature [Eq. (11)]	0.009%	0.009%	0.009%	0.0077%

Operating conditions from M.J. Longeot, P.F. Peterson, personnel communication, 1996.

higher than those of room temperature water, as shown in Table 1. To reproduce the surface tension number of lithium, the temperature of water was raised to 80°C to reduce fluid viscosity [7]. However, using hot water to simulate liquid lithium was unsuccessful and showed opposite trend to the theoretical prediction. The experiments concluded that further analytical and experimental research is required to explain the observed behavior [7]. For flow conditions of high surface tension and Reynolds numbers, the asymptotic wave velocities and wave growth rates as a function of film Reynolds number (given by Anshus [6]) are shown in Fig. 3. The results indicate that to reproduce the wave growth rate of a lithium film with hot water would require much higher liquid velocities which makes the simulation impossible. This simple calculation illustrates that achieving certain fluid conditions, such as Reynolds number, does not guarantee prototypical fluid flow characteristics. In fact, achieving one fluid flow parameter may negatively impact other important flow characteristics because of the interdependence these parameters have on each other. However, for the purpose of characterizing film flow wave development, sodium, which has almost the same surface tension number of lead, a low vapor pressure and a low melting point of 97°C appears to be a good practical simulant for lead in laboratory experiments.

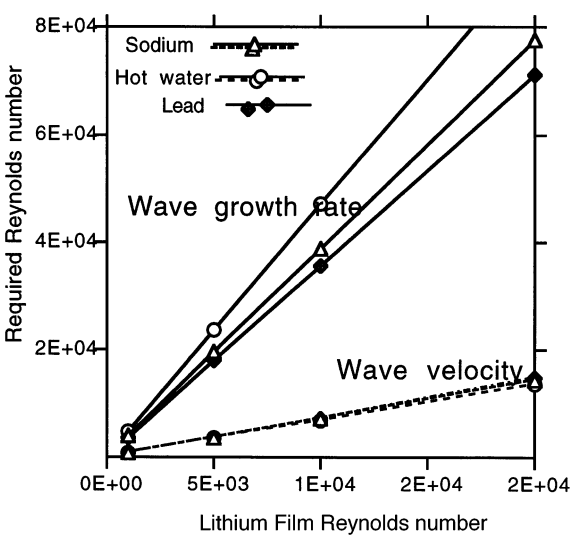

Fig. 3. Reynolds numbers required to simulate prototypical turbulent lithium film wave growth rate and velocity.

The magnitude and uniformity of the film thickness was critical for the Prometheus design because it determined the local wall temperature which impacted the clearing of the cavity. In Prometheus, the following semi-empirical equation was used for the turbulent mean film thickness [8].

$$\delta = 0.136\left[\frac{\nu^2}{g}\right]^{1/3}\mathrm{Re}^{0.583} \tag{7}$$

This correlation is plotted as a function of Reynolds number for various fluids in Fig. 4. The calculations show that for the same Reynolds number, lead produces the thinnest film while Flibe produces the thickest for the liquids consid-

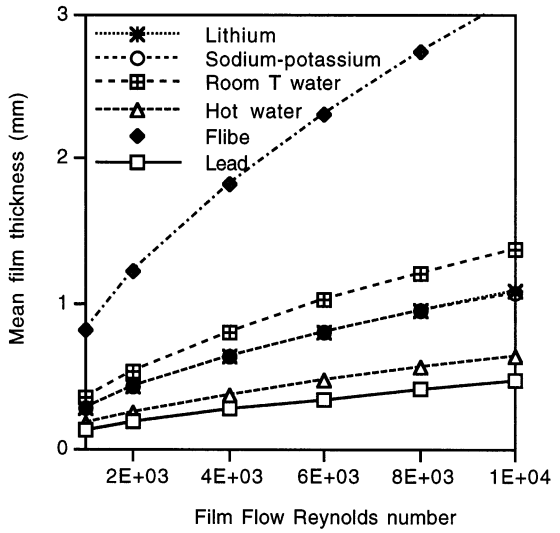

Fig. 4. Mean turbulent film thickness versus film flow Reynolds number for different working fluids.

ered here. The sodium–potassium eutectic alloy gives an exact film thickness of that of liquid lithium and the cool water film is expected to be thicker than the hot water film. However, the room temperature water needs to run at lower velocity to produce prototypical liquid metal films. Moreover, experimental water data has shown that the instantaneous film thickness could change by as much as 250% above and 50% below the mean thickness [9]. This type of surface roughness has yet to be seen experimentally with liquid metals.

3. Thick liquid wall protection schemes

A thick liquid wall protection scheme utilizes continuously flowing, horizontal and vertical, neutronically thick liquid jets facing the fusion region to slow down and stop most of the neutrons before they damage the solid structural material behind the liquid layer [4]. These jets will not function adequately if they disintegrate above their two-meter fall distance to the bottom of the fusion chamber. Even without complete breakup, jet spreading and surface roughness must remain sufficiently controlled in order not to interfere with target injection and beam propagation.

3.1. Curvature of jet surface protuberances

One of the flow configuration requirements regarding thick liquid wall protection schemes is associated with jet surface ripple in which only a small protuberance (± 20 mm over a 10–30 cm wide slab) can be tolerated in order not to block the beam path. Experimental results at reduced pressures (as low as 0.1 atm) indicate that these protrusions are due to turbulence eddies within the jet, and not to waves set up by the relative movement of the ambient air and the shear between the waves and cover gas [10]. According to Levich's basic postulates [11], the dynamic thrust of an eddy (ρV_0^2) is opposed, at the free surface, by the surface tension, σ, associated with the bulge of the surface caused by the approaching eddy:

$$\rho V_0^2 = \frac{2\sigma}{R} \tag{8}$$

where V_0 is the characteristic turbulence eddy velocity and R is the radius of curvature of the deformation of the surface. The turbulence eddy velocity V_0 is defined as (wall friction/ρ)$^{1/2}$ and may be approximated by the Blasius equation:

$$V_0 = 0.2V\,\mathrm{Re}^{-1/8} \tag{9}$$

where V is the mean jet velocity. Substituting Eq. (9) into Eq. (8), the radius, R, of deformation curvature at the surface caused by the eddy can be estimated as:

$$R = \left[\frac{2\sigma}{\rho V^2}\right]\mathrm{Re}^{1/4} \tag{10}$$

or in a non-dimensional form:

$$\frac{R}{D} = \frac{2}{\mathrm{We}}\,\mathrm{Re}^{1/4} \tag{11}$$

where We is the jet Weber number and D is the size of the jet.

In this case, the dimensionless jet surface ripple size can be maintained by simultaneously preserving prototypical jet Reynolds and Weber numbers. However, to what degree the jet size and shape affect the ripple size remains to be studied. The results, shown in Table 2, indicate that the non-dimensional curvature of the water jet surface

protuberance to be observed in the ongoing experiments (M.J. Longeot, P.F. Peterson, personnel communication, 1996) is expected to be 15% less than that of a Flibe jet under reactor operating conditions. Unfortunately, the experiment was not able to demonstrate this because of a jet spread out due to experimental difficulties associated with cavitation (M.J. Longeot, P.F. Peterson, personnel communication, 1996).

3.2. Cavitation phenomena in relation to experimental liquid simulant

The vapor pressure of the liquid will give rise to a certain amount of evaporation into the ambient medium. This is a complicated process, where the mass transfer is strongly affected by the fluid dynamics near the liquid–gas interface. If the ambient pressure is below the vapor pressure of the liquid, the creation of bubbles, or flashing, may lead to violent disruptions of the jet. To eliminate this complication, liquids having vapor pressures sufficiently low to ensure that evaporation will be insignificant should be used. In most laboratory scaled jet flow experiments, water was used as a simulant fluid and operated at prototypical Reynolds and Weber numbers to achieve dynamic similarity. The problem involved with the use of water for jet flow experiments under subatmospheric conditions relates to water cavitation/bubble formation. According to the experimental results of [12], cavitation of water began when the cavitation number ϖ decreased to about 0.4. For this purpose the cavitation number is defined as:

$$\varpi = \frac{(P - P_v)}{0.5\rho V^2} \tag{12}$$

where: P = the local pressure around the jet, P_v = vapor pressure of water at test temperature. Fig. 5 shows the water cavitation number as a function of jet velocity for different chamber pressures and coolant temperatures. The results indicate that it is difficult to operate a water jet flow experiment at a typical reactor fluid velocity of 12 m s^{-1} under a pressure of 0.4 atm without introducing flashing of the liquid. Reducing the coolant operating temperature reduces the coolant vapor pressure, but it does not help prevent cavitation at low operating pressures.

The scaling issue that arises is how to anticipate the onset of cavitation in one liquid based on data obtained for another. Clearly the literature contains a great deal of data on water, however changing the velocity in an attempt to maintain Reynolds number scaling will change the cavitation number. To recover the desired conditions, one must then change the ambient pressure level, which will alter the nuclei density, and since the nuclei play a key role in determining cavitation inception, it is not surprising that our current ability to scale from one liquid to another is quite tentative [13].

4. The impact of nozzle design on jet stability

It is known that jet stability is inextricably associated with the total (micro- and macro) velocity distribution at the nozzle exit. The total velocity distribution is the result of an interaction between the physical properties of the jet liquid and the overall geometry of the nozzle and the supply line. The jet velocity profile has to relax into a nearly flat profile at the desired average

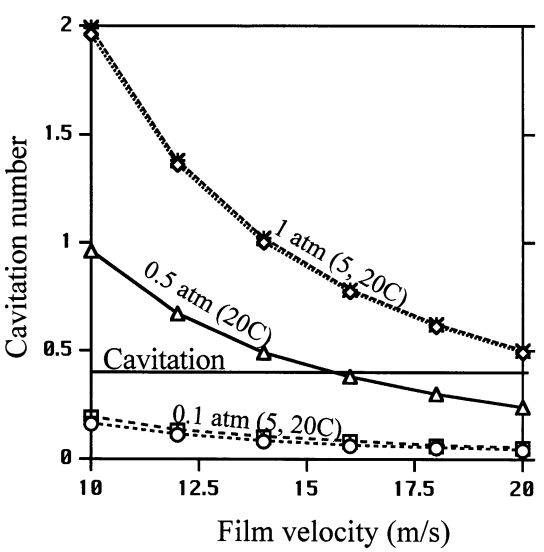

Fig. 5. Cavitation number versus film velocity at different water jet operating conditions.

velocity at the nozzle exit. Hence, there must be an energy redistribution within the jet and the forces resulting from this redistribution presumably play a significant role in the ultimate disintegration of the jet [14]. Jets with fully developed turbulent profiles on exit ($\varepsilon = 1.1–1.2$) are only weakly susceptible to profile relaxation effects, and turbulence may be the deciding factor regarding stability in such cases. Hence, the impact of a specific jet design on the film stability remains a development issue.

5. Conclusions

The present assessment of film flow characteristics have shown the difficulties of using water as a simulant for liquid protectants in experiments conducted to provide the necessary input for evaluating IFE thin and thick liquid wall protection schemes. In particular, according to Levich's basic postulates, the dimensionless jet surface ripple size can be maintained by simultaneously preserving prototypical jet Reynolds and Weber numbers. However, the experimental result of early water jet spread-out demonstrates that there are other effects separate from those due to the Reynolds and Weber numbers. In addition, there are stability parameters characterized by different effects due to the Reynolds number. The calculations have shown that reproducing relevant wave velocities leads to a higher wave growth rate. It is clearly the case that the literature contains a great deal of data on water film flow, and that data on other liquids are quite meager. The assessments show that modified HTS salt seems a good simulant for Flibe and sodium a good simulant for liquid lead fluid. However, in the absence of information on liquids other than water, serious questions remain concerning the issue of scaling. Nevertheless, to best utilize the available R&D resources, further experiments should be performed using fluids having significantly low vapor pressures such as liquid metal or low melting temperature salt or eutectic.

Acknowledgements

This work was performed under US Department of Energy Contract DE-FG0394ER54287.

References

[1] C.J. Cavanaugh, P.F. Peterson, Scale modeling of oscillating sheet jets for the HYLIFE-II inertial confinement fusion reactor, Fusion Technol. 26 (1994) 917.
[2] L.M. Waganer, Innovation leads the way to attractive inertial fusion reactor-Prometheus-L and Prometheus-H, Fusion Eng. Design 25 (1994) 125–143.
[3] W.R. Meier, Osiris, SOMBRERO inertial fusion power plant designs- summary, conclusions, and recommendations, Fusion Eng. Design 25 (1994) 145–157.
[4] R.W. Moir, et al, HYLIFE-II: a molten-salt inertial confinement fusion energy power plant design—final report, Fusion Technol. 25 (1994) 5.
[5] J.E. Howard, On the stability of the flow of thin liquid-lithium films, Nucl. Sci. Eng. 69 (1979) 94–99.
[6] B.E. Anshus, On the asymptotic solution to the falling film stability problem, Ind. Eng. Chem. Fundam. 11 (4) (1972) 502–508.
[7] M.A. Hoffman, W.W. Potts, Experimental behavior of falling liquid films at high surface tension numbers, Ind. Eng. Chem. Fundam. 18 (1) (1979) 27.
[8] J. Gimbutis, A.J. Drobacivius, S.S. Sinkunas, Heat transfer of a Turbulent Water Film at Different Initial Flow Conditions and High Temeprature Gradients, Proceedings 6th International Heat transfer Conference, Toronto, Canada, vol. 1, 1978, pp. 321–326.
[9] H. Takahama, S. Kato, Longitudinal flow characteristics of vertically falling liquid films without concurrent gas flow, Int. J. Multiphase Flow 6 (1980) 203–215.
[10] J.T. Davies, A.A. Young-Hoon, Restrained turbulent jets of a non-Newtonian solution, Chem. Eng. Sci. 29 (1974) 1115–1121.
[11] V.G. Levich, Physicochemical Hydrodynamics, Prentice-Hall, Englewood Cliffs NJ, 1962.
[12] J.W. Hoyt, J.J. Taylor, A photographic study of cavitation in jet flow, ASME J. Fluids Eng. 103 (1981) 14–18.
[13] C.E. Brennen, Cavitation and Bubble Dynamics, Oxford University Press, Oxford, chapters 1 and 2, New York, 1995.
[14] M.J. McCarthy, N.A. Molloy, Review of stability of liquid jets and the influence of nozzle design, Mech. Eng. J. 7 (1974) 1.